Identification of reaction intermediates and mechanism responsible for highly active HCHO oxidation on Ag/MCM-41 catalysts

Dan Chen, Zhenping Qu *, Yahui Sun, Kang Gao, Yi Wang

Key Laboratory of Industrial Ecology and Environmental Engineering (MOE), School of Environmental Science and Technology, Dalian University of Technology, Linggong Road 2, Dalian 116024, China

A B S T R A C T

The adsorption and oxidation mechanism of formaldehyde (HCHO) with time and temperature was systematically investigated by *in situ* FT-IR and mass spectroscopy methods on pure MCM-41 and Ag/MCM-41 catalysts pretreated with different atmospheres (H_2 or O_2). HCHO-TPSR experiments showed that the Ag catalyst pretreated with O_2 was highly active for HCHO oxidation compared with that pretreated with H_2. And it was found by *in situ* FT-IR that the DOM, formate and CO species were the main reaction intermediates for HCHO oxidation on Ag/MCM-41. Importantly, the formation of the formate was not only derived from the HCHO dissociation adsorption by consuming hydroxy group, but also from the disproportionation of DOM active ad-species on Ag/MCM-41 catalysts. It was our first observation of the existence of adsorbed CO on the active silver structure by HCHO-TPSR. The formation of the formate and CO on the surface of the catalyst were both promoted after the Ag/MCM-41 was pretreated with O_2 due to the formation of subsurface oxygen species and the stronger interaction of silver with the support. The quantitative analysis of the formate formation and the calculation of reaction rates for HCHO and CO oxidation suggested that the amount of formed formate and the reaction rates for HCHO and CO oxidation showed the positive linear relationship. An possible reaction scheme for HCHO oxidation on Ag/MCM-41 catalyst was also given in this manuscript.

© 2013 Elsevier B.V. All rights reserved.

1. Introduction

The kinetics and mechanism of HCHO interaction with solid surfaces is of particular significance for modeling catalytic processes such as CO hydrogenation, methyl formate and alcohol synthesis, and dehydrogenation of CH_3OH and for controlling indoor pollutant in airtight buildings [1,2]. In the past years, a number of materials, including supported noble metals (Pt, Ph, Pd, Au and Ag) [3–13] and some metal oxides (Co_3O_4, CeO_2, TiO_2, MnO_x and so on) [7,14,15], have been used for the adsorption and oxidation of HCHO. It has been generally accepted that molecular adsorption of HCHO occurs through σ lone pair donation from the oxygen of carbonyl to Lewis acid sites. The carbon of the carbonyl becomes more electrophilic, favoring an attack from nucleophilic surface oxygen ions to form dioxymethylene (DOM) species [11,16,17]. Hydride transfer between two dioxymethylene species give one formate species corresponds to a net Cannizaro disproportionation [14]. At higher temperature, DOM or formate species will be dissociated to the adsorbed CO and adsorbed H (or H_2), and then they are activated with adsorbed oxygen species to form gas phase CO_2. All these findings point out that although HCHO is a relatively simple molecule, its adsorption and surface transformations are very complex.

Decomposition of HCHO on clean surfaces of the metals or metal oxides under UHV and low temperature conditions is very slow, and molecular desorption of the adsorbed phase is the dominant reaction path. However, experiments indicated that preadsorbed surface oxygen on silver catalyzed the HCHO decomposition to CO_2 accompanied by H_2 and H_2O [2,9,10]. Analysis of DRIFTS spectra of the catalytic surface after HCHO decomposition at 493 K suggested that DOM and formate were intermediates in the process leading to CO_2 and CO formation on Ag powder and supported Ag catalyst [9]. On Ag/MnO_x—CeO_2 catalyst, complete oxidation to CO_2 and H_2O at 373 K has been reported, presumably due to the higher concentration of surface oxygen on silver supplied by the supported catalyst [10]. Barteau et al. [11] reported that the formate species could be generated from the interaction between adsorbed HCHO and oxygen atoms chemisorbed on the Ag surfaces. These studies all mentioned the important role of surface oxygen in HCHO catalytic oxidation. In our previous study, we have found that the subsurface oxygen (O_γ) (proved by H_2-TPR and O_2-TPD experiment) strongly influenced the decomposition capability of HCHO into intermediates such as DOM and formate over Ag based catalysts supported on different supports (MCM-41, SBA-15, NaY, SiO_2

---

* Corresponding author. Fax: +86 411 84708083.
  E-mail addresses: quzhenping@dlut.edu.cn, zhenpq@dicp.ac.cn (Z. Qu).

and TiO_2) [18]. However, it is still uncertain for subsurface oxygen how to participate in HCHO decomposition and oxidation in silver catalysts, how to affect the generation path of reaction intermediate species, particularly which kinds of intermediates. It has been known that the pretreatment of the Ag/SiO_2 catalysts at different atmospheres/temperatures played an important role in the formation of the active silver structure and CO catalytic oxidation [19]. So in this work, the different pretreatment with oxygen and hydrogen for Ag/MCM-41 was conducted to investigate the effect of the silver structure on the HCHO oxidation.

Formate has been found to be the predominant adsorbed intermediate in HCHO decomposition on a series of surface oxides [14]. In the case of Pt/TiO_2 catalyst, generally speaking, adsorbed HCHO is oxidized into surface DOM species followed by formate species through Cannizzaro-type mechanism [3,20]. However, Kiss et al. [6,21] revealed that the formate formation was not the results of Cannizzaro reaction of DOM, and it was generated from the formic acid that was formed by H transformation of DOM species on Pt/TiO_2 and Au/TiO_2 by FTIR and mass spectrometer. The same techniques were also applied to study the HCHO adsorption and reaction on TiO_2 and TiO_2 supported Rh catalysts in 2004 [22]. They found that at high temperatures molecularly adsorbed HCHO and DOM species decomposed to formate [22]. Similarly, Mao et al. [9] also found that DOM decomposed or oxidized to form formate groups at high temperature on Ag powder and supported Ag catalysts. Barteau et al. [11] reported that the formate species were generated from the interaction between adsorbed HCHO and oxygen atoms chemisorbed on the Ag surfaces. This behavior was also observed in the IR study of formic acid adsorption on Ag/SiO_2 [23]. In addition, molecular modeling using periodic density functional theory (DFT) has identified the intermediates and reaction pathways in the dehydrogenation of HCHO on the clean and preoxidized Ag(1 1 1) surface [2]. The intermediates DOM, formate are chemisorbed through the bridge sites, whereas CO and CO_2 are weakly adsorbed with no strong preference for a particular surface sites on clean Ag(1 1 1) slabs [2]. So it is important to research the generation path of formate species over Ag catalysts, which will help to design the silver catalysts for low-temperature HCHO oxidation.

In addition, it has been known that the formate ad-species could decompose into adsorbed CO and H_2O, and then CO species reacted with O_2 to produce gas phase CO_2 on Pt/TiO_2 catalysts [3,24]. They thought the conversion of surface formate species to adsorbed CO on the catalysts was the rate-determining step for the catalytic oxidation of HCHO. However, the research about CO formation and its structure dependence are very rare over Ag catalyst. As early as 1995, the analysis of DRIFT spectra for the HCHO decomposition at 493 K suggested that DOM and formate species were intermediates on Ag powder and supported Ag catalysts during the process of HCHO adsorption, and only CO_2 was formed during HCHO oxidation on Ag powder and silica supported Ag after heating [9]. The significant CO formation was only observed in the presence of α-Al_2O_3, it was thought that CO formation was directly related to alumina surfaces rather than Ag surface.

In view of the previous studies, we can deduce that it is important for HCHO oxidation to study the formation and decomposition path of reaction intermediates, especially formate and CO. Therefore, a fundamental understanding of HCHO behavior over silver catalysts requires a detailed analysis of the identification of reaction intermediates, the elementary reaction step of HCHO decomposition on Ag catalyst. Herein, *in situ* FTIR, Mass spectra, Temperature programmed techniques, such as temperature programmed surface reaction (TPSR) were used to study the characteristics of HCHO adsorption and reaction on the Ag/MCM-41 catalyst in this manuscript. Oxygen and hydrogen pretreatment were also conducted to investigate the effect of the structure

of silver catalyst for the adsorption and oxidation of HCHO. In particular, the quantitative analysis of intermediates combining with the FTIR spectra were used in this paper which will help us to understand the importance of the formation and decomposition of formate ad-species in HCHO adsorption and surface reaction.

2. Experimental

2.1. Catalyst preparation and characterization

MCM-41 supported silver catalysts (Ag/MCM-41) were prepared by impregnation of MCM-41 (Shanghai Zhuoyue Chemical Agent Co., China, S_{BET} = 538.8 m^2/g) with an aqueous solution containing $AgNO_3$, followed by drying at room temperature overnight then drying at 100 °C for about 24 h. The catalysts were sieved into 20–40 mesh granule and then pretreated in flowing O_2/Ar (30 vol.% O_2) or H_2 (99.999%) at 500 °C for 2 h before testing.

H_2-TPR was carried out on the Quantachrom Automated Chemisorption Analyzer. A 0.1 g sample was pretreated with different atmospheres, then cooled to room temperature in a flow of Ar in a fixed bed reactor. For the H_2-TPR study, it was exposed to a flow of 30 mL/min H_2/Ar (10 vol.% H_2) mixture. The temperature was programmed with a constant heating rate of 10 °C/min. X-ray photoelectron spectroscopy was measured using an X-ray photoelectron spectrometer (ESCALAB250, Thermo VG, American) with a monochromatic X-ray source of AlKa (1486.6 eV) under ultra-high vacuum. The binding energies were calibrated internally by the carbon deposit C1s binding energy (BE) at 284.6 eV. The ICP-AES were used to determine the actual content of silver in the synthesized samples, which was performed on an OPTIMA 2000.

2.2. HCHO temperature programmed studies

The HCHO temperature programmed experiments were performed in a fixed catalytic reactor system in the middle of which 0.1 g catalyst (20–40 mesh) was packed. The reaction was performed at temperatures ranged from room temperature (RT) to 500 °C. A thermocouple was placed in the middle of the catalyst bed in the temperature measurement. Gaseous HCHO was generated by flowing He over trioxymethylene (99.5%, Acros Organics) in an incubator kept in an ice water mixture. A HCHO adsorption breakthrough curve was obtained for each run to ensure the adsorption saturation of HCHO over the catalyst surface by the mass spectrum (Ametek, LC-D200M). The catalyst was purged with high purity helium for 1 h to fully remove physically adsorbed HCHO, and then the temperature was ramped at 10 °C/min from RT to 500 °C in a flow of O_2/Ar (30 vol.% O_2) for HCHO-TPSR and in a flow of He for HCHO-TPD. The effluent from the quartz reactor was analyzed by MS. The exhaust line from the reactor to the mass spectrometer was maintained at ~120 °C to prevent the condensation of the HCHO.

2.3. In situ FTIR

In situ FTIR spectra were recorded in BRUKER VERTEX 70 by using variable-temperature quartz cells. A catalyst pellet (12 mm × 0.1 mm in size and 30 mg in weight) was placed in the flow IR cell-reactor and then pretreated in He flow at 300 °C for 40 min. All spectra were recorded with a resolution of 4 cm^{-1} and accumulating 16 scans. A background spectrum was subtracted from each spectrum respectively.

2.4. Quantifying formate species ($HCOO^-$)

The amount of formate species ($HCOO^-$) were determined by ion chromatography using a conductivity detector (Shimadzu SCL-10ASP, Japan). To get the amount of formate ad-species formed

on the catalysts, HCHO was adsorbed for 60 min on the sample of 0.1 g to ensure the adsorption saturation on the catalyst surface. Then the catalysts were purged with high purity helium for 1 h to fully remove physically adsorbed HCHO. The effluent gas was detected by the mass spectrum (Ametek, LC-D200M). Finally, the catalysts were dissolved in 10 mL deionized water with continuous ultrasound treatment for 10 min. The catalyst was pretreated with oxygen before HCHO adsorption.

2.5. CO and HCHO catalytic activity test

CO oxidation activity measurements were carried out in a fixed-bed flow reactor at atmospheric pressure and with 0.2 g catalyst. The reactants for CO oxidation were fed with a volume ratio of $He/CO/O_2 = 79/1/20$ at a total flow rate of 30 mL/min, which was controlled by an independent thermal mass flow controller. On-line gas chromatograph (GC 7890, Techcomp, China) with a TCD detector was employed to measure the reactor inlet and outlet effluent gas streams. The 5A molecular sieves column was used to separate oxygen, carbon monoxide.

In this paper, the CO conversion was calculated from the change of the CO concentration:

$$CO\ conversion = \frac{[CO]_{in} - [CO]_{out}}{[CO]_{in}} \times 100\%$$

where $[CO]_{in}$ is the inlet CO concentration and $[CO]_{out}$ is the outlet CO concentration.

HCHO oxidation activity measurements were also carried out in a fixed-bed flow reactor at atmospheric pressure and with 0.2 g catalyst. The total flow rate was 30 mL/min. Gaseous HCHO was generated by flowing Ar over trioxymethylene (99.5%, Acros Organics) in an incubator kept in an ice water mixture. The flow rate passing through the reactor in all the experiments were controlled at 30 mL/min by a mass-flow meter. And the feeding stream consists of a mixture of 500 ppm HCHO, 25 vol.% oxygen and balanced Ar. The effluents from the reactor were analyzed by on-line gas chromatograph (GC 7890II, Techcomp, China) equipped with FID detectors. To determine the exact concentration of produced carbon dioxide, a nickel catalyst converter was placed before the FID detector and used for converting CO_2 quantitatively into methane in the presence of hydrogen. In typical runs, the reaction data was obtained after HCHO oxidation was performed for 1 h in order to achieve the steady state. No other carbon containing compounds except CO_2 in the products were detected for all the tested catalysts. Thus, HCHO conversion was calculated as follows:

$$HCHO\ conversion\ (\%) = [CO_2] / [CO_2]_* \times 100\%$$

where $[CO_2]_*$ is the concentration of CO_2 in the effluent when HCHO is oxidized completely and $[CO_2]$ is the concentration of CO_2 produced at different temperatures.

3. Results

3.1. Mass spectroscopy studies

It has been known that the performance of HCHO adsorption and oxidation greatly varied with the silver structure of Ag catalysts supported on different supports [18]. In order to well understand the effect of the silver structure on the adsorption and oxidation of HCHO, the HCHO surface reaction was conducted on silver catalysts pretreated with oxygen and hydrogen atmosphere, respectively.

Fig. 1 shows the HCHO-TPSR profiles of Ag/MCM-41 catalysts pretreated with H_2 and O_2, respectively. The HCHO surface oxidation activity and the variety of products in different temperature regions can be obviously observed. The gas oxygen only reacted with the HCHO adsorbed on the silver active sites because no
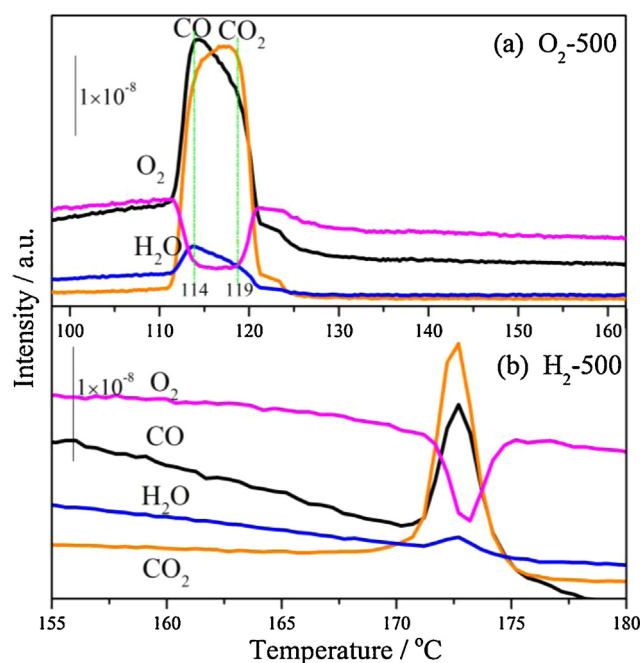

Fig. 1. TPSR profiles of Ag/MCM-41 catalyst pretreated with O_2 and H_2.

oxygen consumption ($m/z = 32$) was observed on MCM-41 silica even at high temperatures in TPSR experiment (not shown here). The obvious gas oxygen consumption ($m/z = 32$) on Ag/MCM-41 catalysts could be observed and meanwhile large amounts of CO ($m/z = 28$), CO_2 ($m/z = 44$) and H_2O ($m/z = 18$) were produced during TPSR experiments. However, a significant difference in the process of oxygen consumption and the formation of CO and CO_2 for the two catalysts should be noticed. Upon heating, the maximum peak for CO formation was observed at 114 °C on the silver catalyst pretreated with oxygen. After that the amount for CO formation obviously decreased, a continuing increase in CO_2 amount was observed. And the maximum value for CO_2 production was obtained at 119 °C. Importantly, a platform for oxygen consumption was observed in the same temperature range of 114–119 °C, which should be closely related to the CO oxidation on the silver catalysts. When the surface reaction temperature was higher than 119 °C, both signals for CO and CO_2 began to decline, and meanwhile the signal for oxygen slowly rose and reached the baseline with the temperature. Compared to the O_2-pretreated Ag catalyst, the pre-adsorbed HCHO could only be oxidized at higher temperature (>170 °C) over H_2-pretreated Ag/MCM-41 catalyst. More importantly, no O_2 consuming platform in a certain temperature range was observed. The oxygen signal was only decreased at temperature higher than 170 °C and then fast increased after 173 °C. It has also been found that the amount for CO and CO_2 formation on the O_2-pretreated silver catalyst was far larger than that on the H_2-pretreated silver catalyst. The silver catalyst pretreated with oxygen showed a better surface reaction activity for HCHO oxidation at low temperature, and the HCHO adsorption and activation was strongly related to the pretreatment conditions of silver catalyst.

3.2. In situ FTIR results

In order to well understand the HCHO adsorption behavior and the intermediate transformation process, *in situ* FTIR experiments were conducted on different samples. The adsorption and reaction process of the studied catalysts could be *in situ* monitored, allowing the study of the adsorption as a function of time, temperature and tracing of each elementary reaction. Before the beginning of
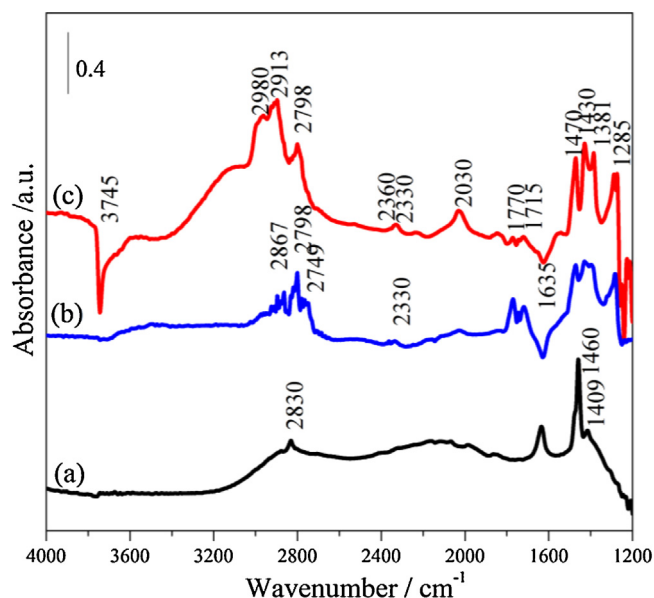
Fig. 2. FTIR spectra of MCM-41 (a), H_2-pretreated (b) and O_2-pretreated (c) Ag/MCM-41 catalysts after exposed to a flow of HCHO + He for 80 min.

FTIR experiments, the samples were swept by He gas for 30 min at 300 °C. The background spectrum was subtracted from each spectrum respectively. So the decrease of the band intensities should be connected with the consumption of reactant species and the increase was connected with its production.

The adsorption spectra of HCHO at room temperature over MCM-41 and Ag/MCM-41 catalysts are presented in Fig. 2. The adsorption of HCHO for 60 min on pure MCM-41 sample caused the appearance of the bands at 1409, 1460, 1635, 2830 cm^{-1}. Additional peaks grew at 1285, 1715, 1770, 2030, 2330, 2360, 2913, 2980 and 3745 cm^{-1} when silver was supported on MCM-41 silica. The peak at 1409 cm^{-1} was divided into two distinct shoulder peaks at 1381 and 1430 cm^{-1} with strong intensity when silver was supported on the MCM-41. Furthermore, the peak at 1460 cm^{-1} shifted to 1470 cm^{-1}, and the peak at 2830 cm^{-1} became detectable at 2798, 2913 and 2980 cm^{-1} for the O_2-pretreated sample and at 2837, 2798 and 2749 cm^{-1} for H_2-pretreated sample. A distinct negative peak at 3745 cm^{-1} was discernible on the O_2 pretreated Ag/MCM-41 catalyst.

The assignment of these bands for our samples have been collected and presented in Table 1. The bands at 1409 cm^{-1} on MCM-41 and 1381, 1430 cm^{-1} on Ag/MCM-41 can be ascribed to υ(OCO) in dioxymethylene (DOM, H_2CO_2). The maximum of

Table 1
Wavenumbers (cm^{-1}) of species associated with HCHO adsorption on MCM-41 and Ag/MCM-41 and their assignments.

Observed wavenumber (cm^{-1})			Assignment
Ag/MCM-41		MCM-41	
O_2-500	H_2-500		
3745	3730		OH stretch
2980	2867		υ_a(OCO) + δ(CH) in formate
2913		2830	υ(CH$_2$) in formate
2798	2798, 2749		υ_s(OCO) + δ(CH) in formate
2330, 2360	2330, 2360	1460	CO$_2$
2030	2028	1409	Adsorbed CO
1770, 1715	1770, 1715		C=O in molecular HCHO
1470	1470		δ(CH$_2$) in DOM
1381, 1430	1399, 1430		υ(OCO) in DOM
1285	1285		υ(CH$_2$) in DOM
1200-1000	1200-1000		Methoxy

1460 cm^{-1} observed on MCM-41 and 1470 cm^{-1} observed on Ag/MCM-41 were certainly assigned to δ(CH$_2$) in DOM. The bands associated with 2700–3000 cm^{-1} could be identified as the features of the formate species (HCOO) with the peaks at 2798 and 2749 cm^{-1} (υ_s(OCO) + δ(CH) in formate), 2913 cm^{-1} (υ(CH$_2$) in formate) and 2980 and 2867 cm^{-1} (υ_a(OCO) + δ(CH) in formate). In addition, the positive bands at 1715 and 1770 cm^{-1} observed on the Ag supported catalysts were assigned to the molecularly adsorbed HCHO (CH$_2$O$_{(a)}$) [9,14,15,25]. The fact that a large amount of DOM and formate species were observed on the Ag/MCM-41 catalysts after HCHO adsorption compared with the pure MCM-41 suggested that the formation of DOM and formate species was significantly promoted due to the silver doping. However, the formation capacity of the DOM and formate species was different on the two Ag/MCM-41 catalysts, and the DOM and formate species easily formed on the O_2-pretreated silver catalyst. In addition, the gas phase CO$_2$ (at 2330 and 2360 cm^{-1}) and adsorbed CO (at 2030 cm^{-1}) were also found on the Ag supported catalyst.

Fig. 3 shows the *in situ* FTIR spectra obtained from a time-dependence study of HCHO adsorption on the O_2-pretreated and H_2-pretreated Ag/MCM-41 catalysts. For O_2-pretreated Ag/MCM-41 catalyst, bands at 1285, 1381, 1430, 1470, 1715, 1770, 1843, 2030, 2330, 2360, 2798, 2913, 2980, 3280 cm^{-1} were observed after HCHO adsorption at room temperature, as shown in Fig. 3(a). Prolonged adsorption time resulted in an obvious increase in the intensity of DOM species on Ag surfaces (1285–1500 cm^{-1}). The enhanced absorbance value of the bands at 2798, 2913, 2980 cm^{-1} suggested that a greater amount of formate species formed with the increase of the adsorption time. The remarkable formation of CO (at 2030 cm^{-1}) and CO$_2$ (at 2330 and 2360 cm^{-1}) were observed after 10 min for HCHO adsorption, moreover they grew in intensity with the increase of the adsorption time. The spectra for HCHO adsorption of H_2-pretreated Ag/MCM-41 were similar to the O_2-pretreated sample. As shown in Fig. 3(b), bands at 1285, 1399, 1430, 1470, 1715, 1770, 2030, 2749, 2798, 2867, 3730 cm^{-1} were also observed after HCHO adsorption at room temperature. The bands in the range of 1200–1600 cm^{-1} attributed to DOM species also increased in intensity with the increase of the adsorption time. Differently, the amount of DOM formed on the H_2-pretreated sample was obviously lower than that formed on the O_2-pretreated sample. Similarly, the amount of formate species (2700–3000 cm^{-1}) formed on the H_2-pretreated sample was also less than that of O_2-pretreated sample. In addition, only a slight increase of adsorbed CO (2030 cm^{-1}) and CO$_2$ species (2330 and 2360 cm^{-1}) was observed. CO and CO$_2$ were easily formed on the Ag/MCM-41 catalyst pretreated with oxygen. Interestingly, an obvious change for the peak at 3745 cm^{-1}, assigned to the surface OH groups, was observed on the silver catalyst pretreated with O_2. It was noteworthy that the intensity of the negative feature at 3745 cm^{-1} was enhanced with the increase of adsorption time, which should be connected with the consumption of the surface OH groups during the interaction of HCHO with the silver catalyst. However, only a slight change of the surface OH was observed on the H_2-pretreated sample.

Fig. 4 shows the dynamic changes of *in situ* FTIR spectra of O_2-pretreated and H_2-pretreated Ag/MCM-41 catalysts as a function of temperature in a flow of O_2. All samples were all pre-adsorbed HCHO before oxygen purging. The bands at 1715 and 1770 cm^{-1} attributed to molecularly adsorbed HCHO disappeared completely after purging with O_2 flow for 60 min on the two Ag/MCM-41 catalysts. During the heating process over the Ag/MCM-41 catalysts, the bands in the range of 1280–1500 cm^{-1} (DOM) decreased with the increase of the temperature. Interestingly, the bands in the range of 2798–2980 cm^{-1} (formate species) showed a little increase with the increase of the temperature initially then decreased with the continuing temperature for the two samples. In the region of 1200–1280 cm^{-1}, 2300–2400 cm^{-1} and 3700–3730 cm^{-1} due to
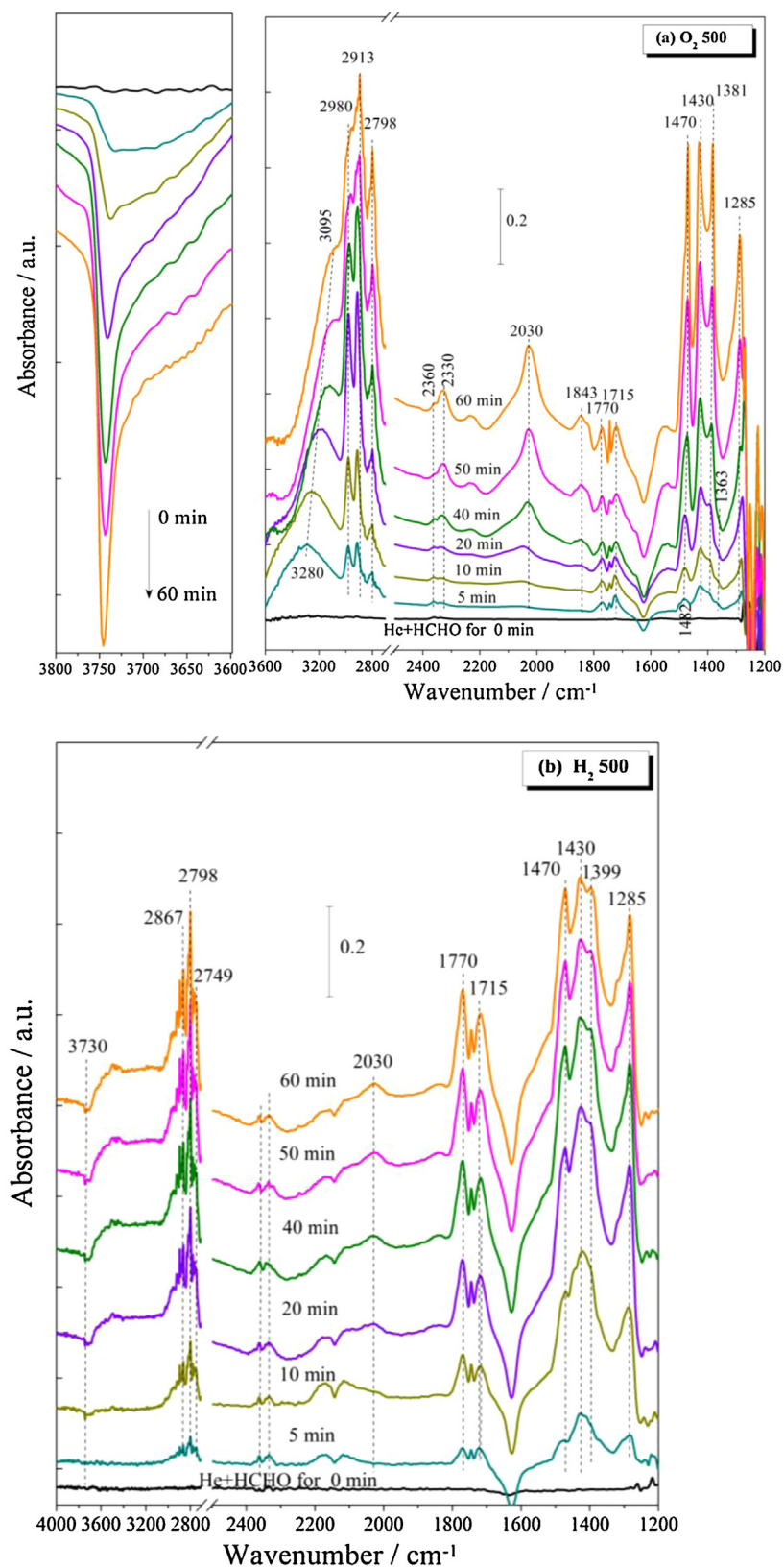
Fig. 3. Dynamic changes of FTIR spectra of O_2-pretreated (a) and H_2-pretreated (b) Ag/MCM-41 catalysts as a function of time in a flow of HCHO + He at room temperature (a, after O_2 pretreatment; b, after H_2 pretreatment).
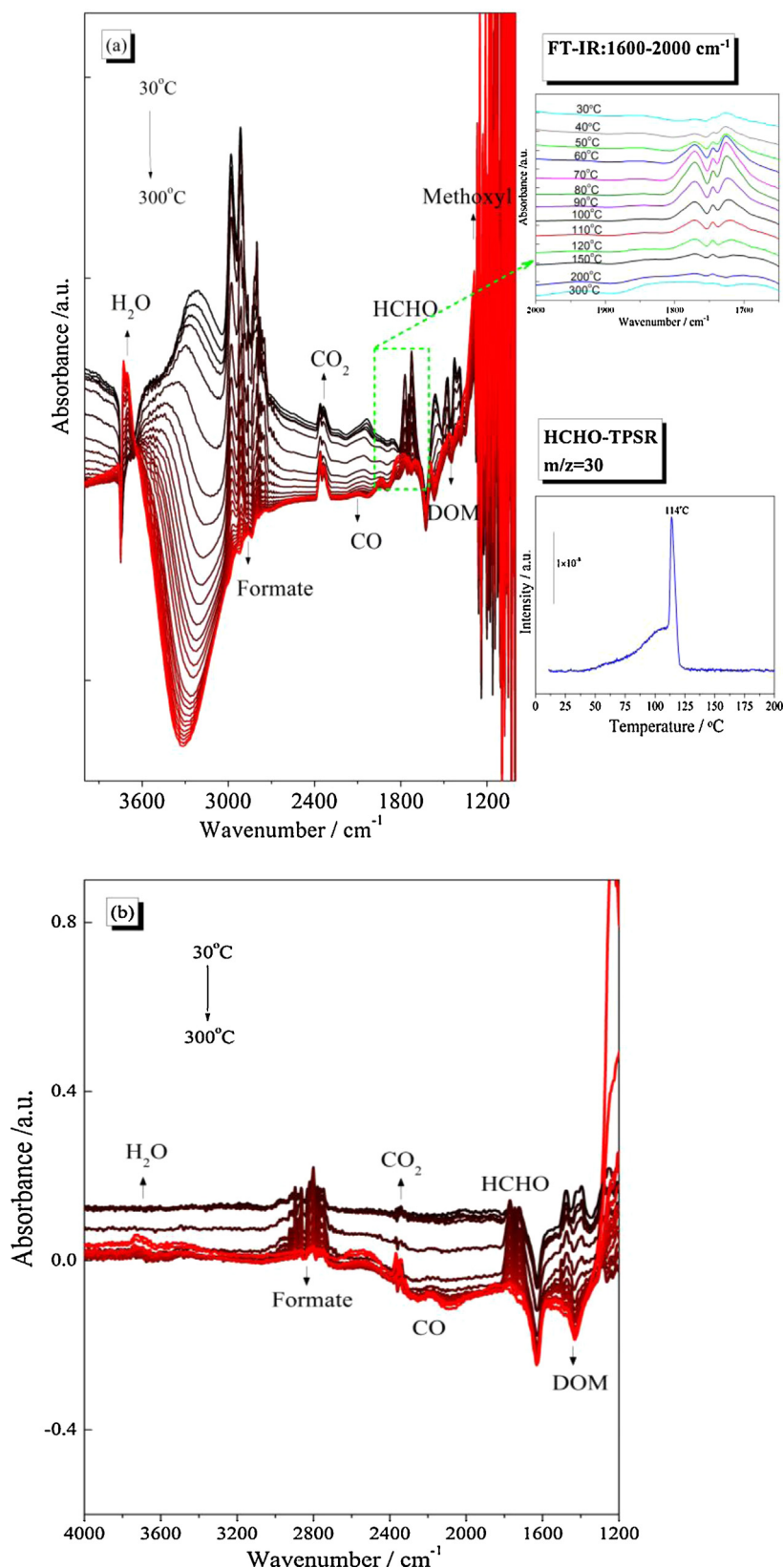
Fig. 4. Dynamic changes of FTIR spectra of O_2-pretreated (a) and H_2-pretreated (b) Ag/MCM-41 catalysts as a function of temperature in a flow of O_2.

methoxyl, CO_2 and H_2O were sharply produced with the increase of temperature on the O_2-pretreated Ag/MCM-41 catalysts (Fig. 4a), while only a little increase was observed on the H_2-pretreated sample (Fig. 4b) was observed.

Another interesting result was the detection of molecularly adsorbed HCHO. The peak for molecularly adsorbed HCHO became visible at 1715 and 1770 cm^{-1} from 50 °C to 120 °C, but vanished at temperature above 120 °C on the O_2-pretreated silver catalyst, as
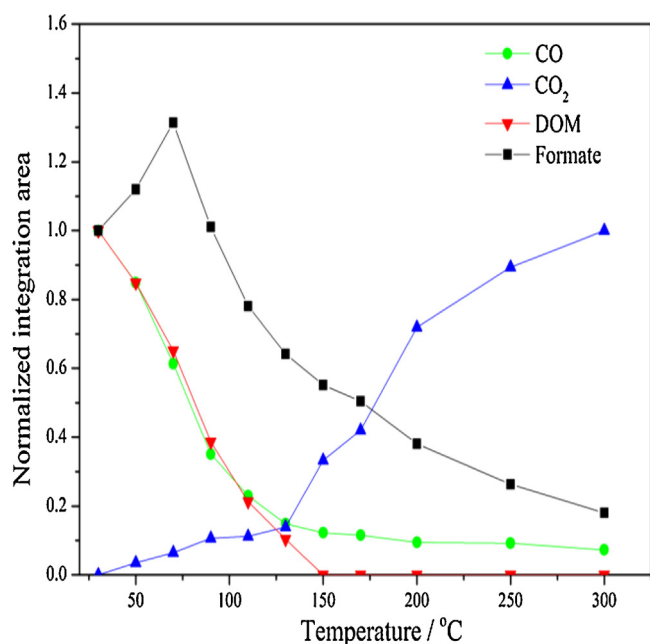
Fig. 5. Temperature dependence of the integrated areas of the peak in the range of 3050–2710 cm^{-1} in a flow of O_2 (■formate species), 2400–2285 cm^{-1} (▲CO_2), 2100–1987 cm^{-1} (●CO), 1622–1363 cm^{-1} (▼DOM) of Ag/MCM-41 catalyst pretreated with O_2.

shown in the upper inset of Fig. 4(a). Actually, no similar observation about the drastic production of molecularly adsorbed HCHO was reported in the previous literatures. The similar result was also intuitively found in our TPSR experiments (in the bottom inset of Fig. 4(a)). In theory, pre-adsorbed HCHO (m/e = 30) would react with O_2 (m/e = 32) in HCHO-TPSR experiment. CO_2 (m/e = 44) and H_2O (m/e = 18) were produced, and meanwhile the adsorbed HCHO and O_2 were consumed. However, HCHO was sharply produced (or desorbed) in the TPSR experiment from 110 °C initially until 114 °C even if O_2 was continuously consumed in the same temperature range.

The integrated areas of IR peaks for the intermediate ad-species in Fig. 4(a) are displayed as a function of temperature in Fig. 5 After the sample was exposed to HCHO for 60 min on the O_2-pretreated Ag/MCM-41 sample, DOM and formate were the dominant surface species on the Ag/MCM-41 surface. And meanwhile a trace amount of the adsorbed CO species formed. With the increase of reaction temperature, the band intensities for DOM and adsorbed CO decreased drastically before 130 °C. Meanwhile, it was worthwhile to note that only a small amount of CO_2 existed before 130 °C on the Ag/MCM-41 catalyst. Interestingly, there was a little formation of formate species in the initial reaction process (50–70 °C) on the sample, and then the amount was sharply decreased during 70–130 °C. After 130 °C, the decrease in intensity of the formate species became milder, and meanwhile more production of CO_2 was observed. For the H_2-pretreated Ag/MCM-41 catalyst, the amount increase of formate intermediates was observed in the range of 50–90 °C, and the decrease in the intensity occurred only after 90 °C (not shown here). The formation and transformation path of the formate species will be discussed in the next section.

4. Discussion

4.1. Dioxymethylene ($H_2CO_{2(a)}$) formation

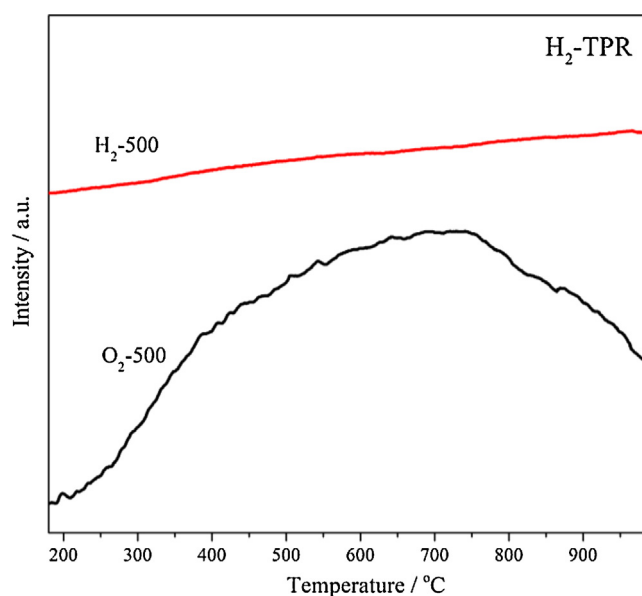The previous findings have pointed out that although HCHO is a relatively simple molecule, its adsorption and surface

Fig. 6. H_2-TPR spectra of Ag/MCM-41 catalysts pretreated with O_2 and H_2.

transformations are very complex [3,5,9,14,15,22,26–29]. In this paper, it was found that adsorbed HCHO could be easily dissociated to DOM on the surfaces of different Ag/MCM-41 catalysts even on the pure MCM-41 during the HCHO adsorption at room temperature. However, not all DOM ad-species were active for HCHO oxidation because no surface oxidation activity on pure MCM-41 was observed. In order to well distinguish the DOM ad-species formed on pure MCM-41 and active silver catalysts, we denoted $H_2CO_{2(a)}$ as that formed on pure MCM-41 and $H_2CO_2-Ag_{(a)}$ as that formed on supported silver catalysts.

$$HCHO_{(a)} + O \rightarrow H_2CO_{2(a)} \tag{1-1}$$

$$HCHO_{(a)} + O + Ag_{(s)} \rightarrow H_2CO_2-Ag_{(a)} \tag{1-2}$$
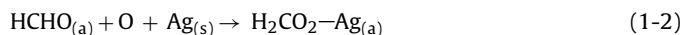
4.2. Formate formation on the Ag sites ($HCOO-Ag_{(a)}$)

As observed, a large amount of DOM and formate species were observed on the Ag/MCM-41 catalysts after HCHO adsorption compared with the pure MCM-41. The formation of DOM and formate species was promoted due to the silver doping, and this kind of acceleration action was more remarkable for O_2-pretreated silver catalyst. Thus it was reasonable to suggest that the formation of formate ad-species was associated with the silver doping and the pretreatment condition for the silver catalyst. Barteau et al. have reported that the generation of the formate species was resulted from the interaction between adsorbed HCHO and oxygen atoms chemisorbed on the Ag surfaces [11]. It has been known that the pretreatment of the Ag/SiO$_2$ catalysts with oxygen at high temperature would result in the formation of subsurface oxygen, which affected the CO catalytic oxidation activity of the silver catalysts [19]. Fig. 6 shows the H_2-TPR of Ag/MCM-41 catalysts pretreated with H_2 and O_2. A broad reduction peak higher than 200 °C was observed for the O_2-pretreated catalyst, which was attributed to subsurface oxygen species (O_γ) associated with O_2-TPD experiments in our previous studies [18,30]. This particular silver-oxygen species did not appear on the surface of H_2-pretreated Ag/MCM-41, which may be the reason for the low formation ability of formate species. Thus the particular silver-oxygen structure really played a key role in the formate ($HCOO_{(a)}$) formation and then the activity for HCHO oxidation.
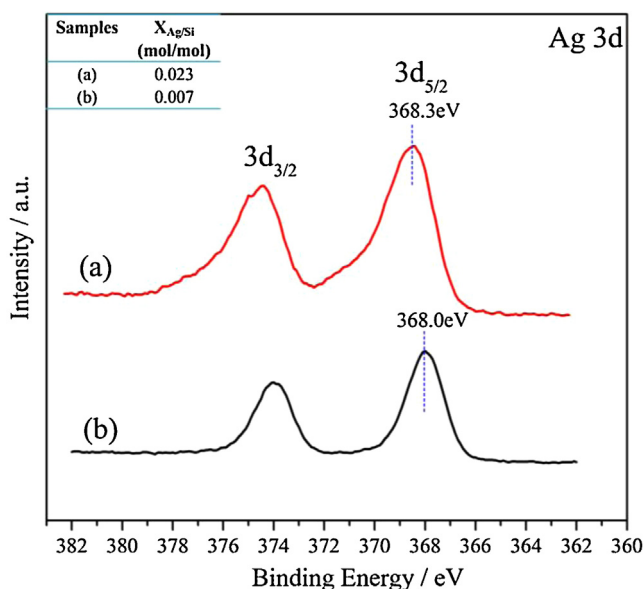
Fig. 7. XPS spectra of Ag/MCM-41 catalysts pretreated with O_2 (a) and H_2 (b).

As we all know, the pretreatment will influence not only the oxygen species but also the silver valence state and the interaction of Ag with support. In order to well investigate the chemical state of the silver species, the Ag 3d photoelectron spectra of the different silver catalysts are presented in Fig. 7. As shown in Fig. 7, two apparent XPS peaks can be observed between 360 and 380 eV of the binding energy for Ag 3d, due to the removal of electrons from the $3d_{3/2}$ and $3d_{5/2}$ core levels [31]. When the silver catalyst was pretreated with H_2, the Ag 3d peak at 368.0 eV was observed (Fig. 8(b)), which can be assigned to Ag metallic state [32,33]. Differently, the BE of the metal Ag $3d_{5/2}$ shifted to the higher value (368.3 eV, Fig. 7(a)) when the Ag/MCM-41 was pretreated in O_2. The positive shift of the Ag (3d) binding energies showed that the silver nanoparticles have a greater tendency to gain electron after O_2 pretreatment. That was to say that there may exist the electron transfer between Ag and the support, and the stronger interaction between

Fig. 8. HCHO-TPD profiles over Ag/MCM-41 catalyst pretreated with oxygen (a) and hydrogen (b).

silver species and the support formed after the silver catalyst was pretreated with O_2 at 500 °C [34]. The use of XPS intensity ratios of metals to that of the support will further provide the information regarding the dispersion degree of the active metals on the support surface. And the surface Ag/Si mole ratios obtained from the XPS result are shown in the insert tables of the Fig. 7. It was found that the surface Ag/Si ratio steadily decreased from 0.023 for oxygen pretreatment to 0.007 for hydrogen pretreatment. More silver particles existed on the surface of the support after O_2 pretreatment, and H_2 pretreatment led to the migration of silver particles from the surface to the bulk [35,36]. The stronger interaction and the well dispersed silver nanoparticles on the surface after oxygen pretreatment could be beneficial for the HCHO adsorption, and the adsorption amount of HCHO was obviously enhanced after oxygen pretreatment (as shown in TPD patterns of Fig. 8(a)).

In addition, a very interesting correlation can be drawn between formate formation and hydroxyl group consumption on these studied samples. It is known that the FTIR signals of −OH might be resulted from the −OH on the support surface and resulted H_2O. However, in our work, the background spectrum was subtracted from each spectrum respectively before HCHO adsorption or oxidation. So the peaks would be negative when the reactants on the surface of the sample were consumed, and otherwise, the peaks for the products would be increased as a positive peak with the time. Thus the negative peak for −OH signal should be thought to be the consumption of the −OH group on the surface of the sample during the HCHO dissociation adsorption process.

With the increase of the adsorption time, the surface concentration of formate was strongly enhanced; meanwhile the concentration of OH group was sharply decreased. And no obvious consumption for hydroxyl group was observed over pure MCM-41 and H_2-pretreated Ag/MCM-41 samples (Figs. 2 and 3). The important depletion for the surface hydroxyl group was only observed on Ag/MCM-41 catalyst pretreated with oxygen during the formation of formate species at room temperature. So it can be written as follows:

$$HCHO_{(a)} + OH + Ag_{(s)} \rightarrow HCOO-Ag_{(a)} + 2H \quad (2)$$
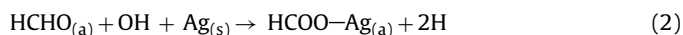
We denoted the particular silver-oxygen structure as $Ag_{(s)}$ in this paper.

Fig. 9 shows the Arrhenius plots of HCHO oxidation rates per gram Ag catalyst over Ag/MCM-41 catalysts with different silver loadings in the temperature of 30–50 °C. The reaction rates of HCHO oxidation are defined as the mole of HCHO molecules converted per gram Ag catalyst per second ($mol_{(HCHO)} g_{(catal)}^{-1} s^{-1}$) at a certain temperature. As shown in Fig. 9, the reaction rate increased monotonically with the increase of the Ag loading from 0.80% to 4.92%, however, the further increase of the silver loading to 8.85% resulted in the decrease of the reaction rate. The HCHO oxidation specific reaction rate at 50 °C on Ag/MCM-41 catalysts can be also found in Table 2. The reaction rate for HCHO oxidation strongly depended on the variation of the silver loading, which was possible due to the existence of different fractions of silver species as silver loading on the support varied [37].

The above discussion in Section 4.2 has shown that the formation of formate species and the following the activity of HCHO oxidation may be related with the formation of subsurface oxygen of silver catalyst. Thus in our experiments, the amount of subsurface oxygen on the Ag/MCM-41 catalysts with different silver loadings has been compared according to the H_2-TPR results, and the results are shown in Table 2. Similarly, it was also found that the amount of subsurface oxygen species was increased with the silver content to 4.92%, and then decreased with the further increase of the silver loading. The trend of the subsurface oxygen in the samples was proportional to the HCHO catalytic oxidation reaction rates, as
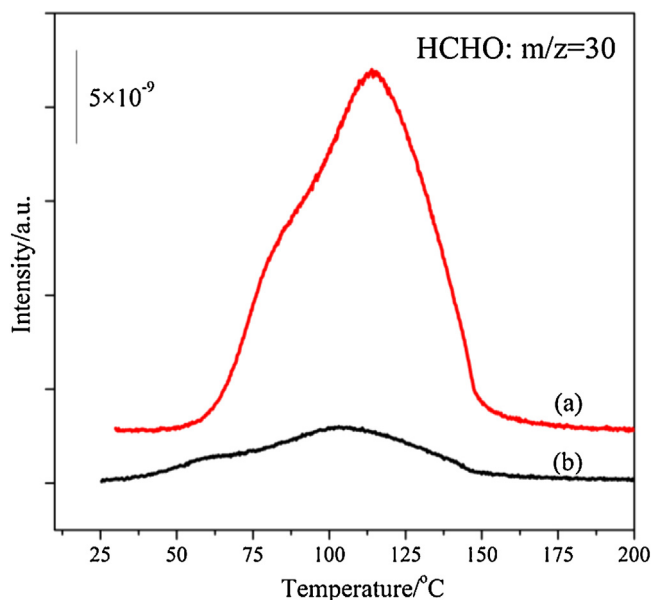
Table 2
Rate$_{HCHO}$, Rate$_{CO}$ and the adsorbed formate amount of different samples.

Samples[a]	Rate$_{HCHO}$ × 10^{-6} [b] (mol$_{(HCHO)}$ g^{-1}$_{(catal)}$ s^{-1})	Rate$_{CO}$ × 10^{-6} [c] (mol$_{(CO)}$ g^{-1}$_{(catal)}$ s^{-1})	Adsorbed formate amount[d] (ppm)	O$_\gamma$ amount[e] (μmol g^{-1})
0.80Ag/MCM-41	4.464	0.065	24.6	106.8
2.77Ag/MCM-41	6.082	0.082	37.4	196.6
4.92Ag/MCM-41	8.482	0.316	44.4	226.9
8.85Ag/MCM-41	4.399	0.155	17.3	135.0
10.01Ag/MCM-41	4.957	0.221	11.5	152.0

[a] Ag content was obtained from ICP results.
[b] The Rate$_{HCHO}$ here was calculated by the moles of HCHO converted on the per gram Ag catalyst per second at 50 °C.
[c] The Rate$_{CO}$ here was calculated by the moles of CO converted on the per gram Ag catalyst per second at 30 °C.
[d] Calculated from the IC results.
[e] Calculated from H$_2$-TPR results.

shown in Fig. 10. This directly proved that the formation of subsurface oxygen species indeed played an essential role in the HCHO oxidation reaction.

Actually, the quantitative analysis about the formate formation combining with the FTIR spectra would help us to well understand the importance of the formate ad-species in HCHO adsorption and surface reaction. The amount of formate species formed on the silver catalysts with different loading during HCHO adsorption at room temperature was quantified by ion chromatography, and the results are shown in Table 2 and Fig. 11. Interestingly, the formation of formate ad-species was well consistent with the silver loading, and its formation amount increased with the increase of Ag content then got the climax on 4.92% Ag catalyst, then decreased with the increase of Ag content from 4.92% to 10.01% subsequently. The formation of formate species and reaction rates for HCHO catalytic oxidation showed the positive linear relationship on silver catalyst. Therefore, it was reasonable to suggest that the formate ad-species were the most stable organic intermediate and its formation would control the reaction rates of HCHO oxidation over Ag catalysts. Moreover its formation was strongly related with the formation of subsurface oxygen species on the silver catalyst.

4.3. Carbon monoxide (CO$_{(a)}$) formation and oxidation

It was our first time observation of CO intermediate by the method of HCHO-TPSR and IR study in HCHO catalytic oxidation
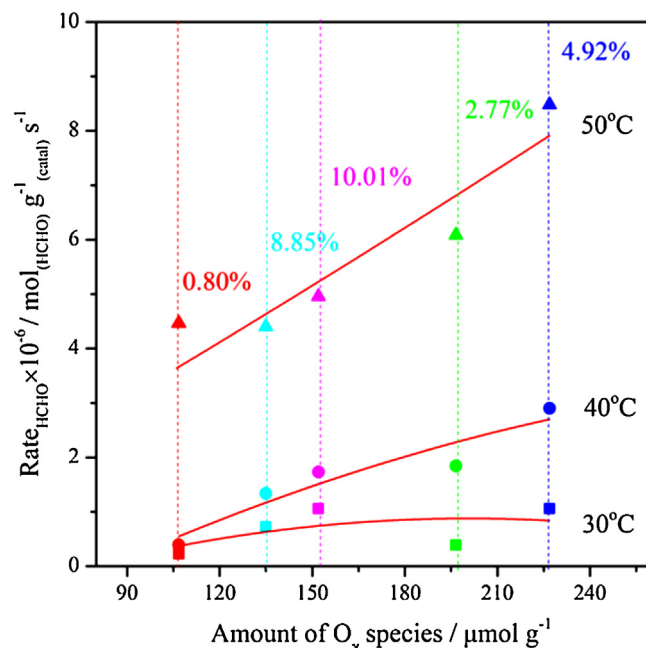

Fig. 10. HCHO oxidation reaction rates determined at 30–50 °C over Ag/MCM-41 with different silver loadings *versus* the amount of subsurface oxygen.
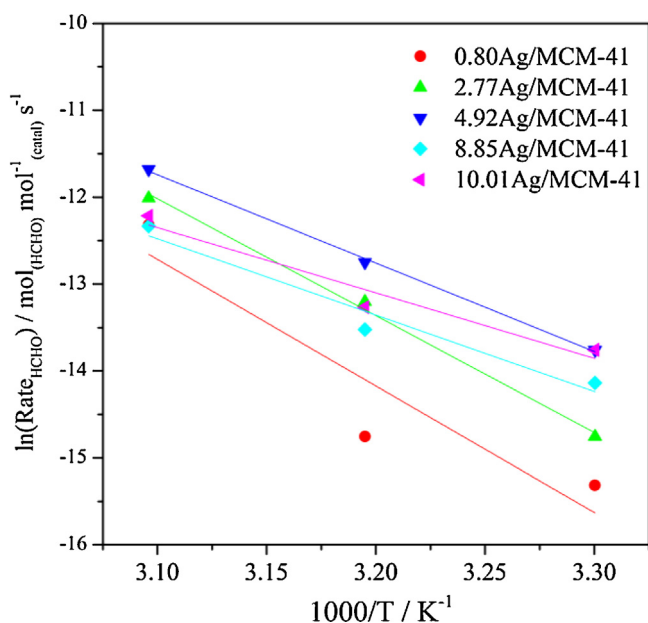

Fig. 9. Arrhenius plots of the HCHO oxidation reaction rates per gram of catalysts at 30–50 °C over Ag/MCM-41 catalysts with different silver loadings.
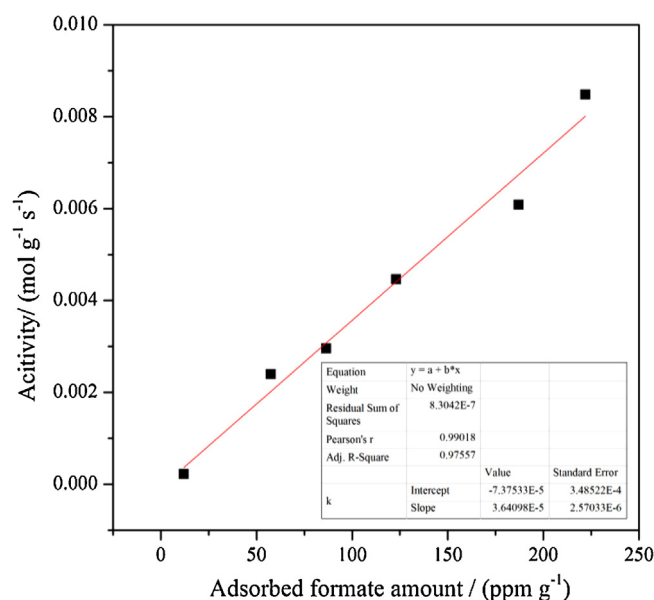

Fig. 11. The linear fitting of adsorbed formate amount per gram catalyst and reaction rates of HCHO oxidation over silver catalysts at 50 °C.

over silver catalysts. As shown in HCHO-TPSR profiles, the fast formation of CO in the initial reaction process was suggested to be the reaction pathway of the decomposition of formate into CO. This process was different from the results reported by Mao et al. about HCHO oxidation on Ag catalysts [9]. They insisted that the CO formation was directly related to HCHO dissociated adsorption over alumina surfaces rather than Ag surface. In our case, CO formation was not found on the pure support MCM-41. Thus the CO formation should be associated with the Ag surface. On the basis of the results, the surface formate active species decomposed into adsorbed CO and H_2O:

$$HCOO-Ag_{(a)} + H \rightarrow CO-Ag_{(a)} + H_2O_{(g)} \qquad (3)$$
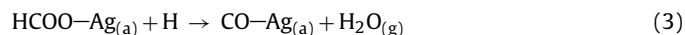
In addition, this $CO-Ag_{(a)}$ could be oxidized into the gas phase CO_2 after purging with O_2 even at room temperature (proved by FTIR). The enhanced gas phase CO_2 in O_2 purging process strengthens this conclusion:

$$CO-Ag_{(a)} + O \rightarrow CO_{2(g)} \qquad (4)$$

Here the formation of CO and formate was all observed in the Ag/MCM-41 samples. Moreover, their formation was all strengthened after the silver catalyst was pretreated with oxygen. Thus, the formed subsurface oxygen structure and stronger interaction of silver and support promoted the formation of CO and formate species, and the following oxidation or decomposition. In order to well understand the relation of CO oxidation with the HCHO oxidation, CO oxidation on the fix-bed was also conducted. The calculated reaction rates of CO and HCHO oxidation in the silver catalysts are shown in Table 2. The same variation tendency of the reaction rates for HCHO and CO oxidation was found on the different silver catalysts. Therefore, it was reasonable to think that CO oxidation was an essential step in the HCHO oxidation.

4.4. Another formation path of formate (HCOO$_{(a)}$)

Another interesting result was that the formate formation was not only derived from the HCHO$_{(a)}$ dissociation along with OH group consumption but also from the disproportionation of DOM active ad-species on Ag/MCM-41 catalysts. As shown in Fig. 5, it has been found that there is a little increase in the band intensities of formate species in the initial reaction process (50–70 °C) on O_2-pretreated Ag/MCM-41 catalyst, then the amount of formate species sharply decreased during 70–130 °C. The formation of methoxyl ($H_3CO_{(a)}$, at 1200–1000 cm^{-1}) has also been found in the heating process. Thus it could be assumed that the DOM disproportionation occurred on the Ag/MCM-41 catalysts [14]:

$$(5) 2H_2CO_2-Ag_{(a)} \rightarrow HCOO-Ag_{(a)} + H_3CO_{(a)}$$
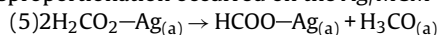
In addition, the sharp increase of gas CO_2 in the intensity after 130 °C (Fig. 5) and the observation of H_2 in TPSR experiment (not shown here) also suggested that heating up the reaction temperature can also result in the direct decomposition of parts of formate intermediates:

$$HCOO-Ag_{(a)} \rightarrow CO_{2(a)} + H_{(a)} \qquad (6)$$

$$2H_{(a)} \rightarrow H_{2(g)} \qquad (7)$$

Taking these results into account, we believed that the formed rate of formate species was far greater than the decomposed rate at relative low reaction temperature, which resulted in the sharp growth of integrated areas for formate species. However, with the increase of the temperature, the rate of formate which was oxidized into CO_2 exceeded the formate formation rate. More CO_2 formation was obviously observed.
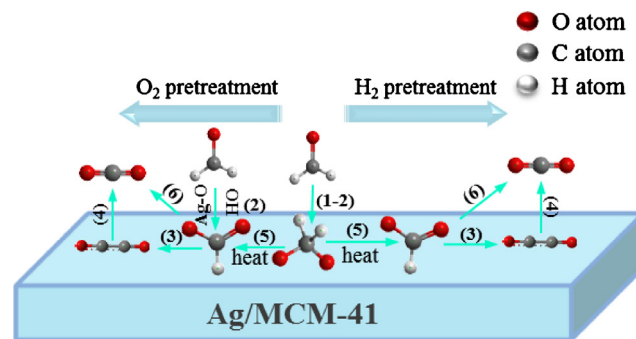

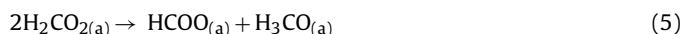**Fig. 12.** Scheme of HCHO adsorption and oxidation over Ag/MCM-41 catalysts.
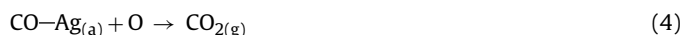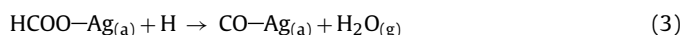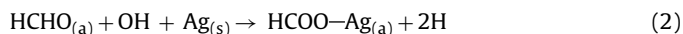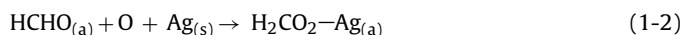
4.5. Molecularly adsorbed HCHO (HCHO$_{(a)}$)

It has been found an increase of molecularly adsorbed HCHO in IR intensity in O_2 flow in the temperature range of 50–120 °C over O_2 pretreated samples (Fig. 4(a)). In theory, the gas oxygen would react with the adsorbed HCHO to form CO_2 and H_2O during TPSR experiment, and the oxygen and HCHO would be consumed at the same time. However, a little amount of HCHO ($m/z = 30$) was still observed in TPSR experiment when gas phase O_2 was consumed over O_2 pretreated Ag/MCM-41 catalysts, as shown in the bottom inset of Fig. 4(a). It has been known that the formate and CO intermediates formed on the Ag active sites were active, which was finally oxidized into CO_2 and H_2O with the increase of reaction temperature. Therefore, the formed molecular HCHO on Ag/MCM-41 catalysts in O_2 flow in the heating process (from 50 °C to 120 °C) should be related with the inactive intermediates formed on the MCM-41 support. As a result of only DOM formed on the pure MCM-41 support catalysts, the gas HCHO should be resulted from the decomposition of DOM species. That was:

$$H_2CO_{2(a)} \rightarrow HCHO_{(a)} + O \qquad (8)$$

4.6. Elementary reaction steps of HCHO oxidation over Ag/MCM-41

Therefore, a potentially important revelation of HCHO dissociated adsorption and oxidation with time and temperature over Ag catalysts was proposed in this paper. In summary, the addition of silver to MCM-41 resulted in some interesting observations on the HCHO catalytic oxidation reaction. A simple possible pathway (Fig. 12) of molecular HCHO adsorption and oxidation was given in detail over the Ag/MCM-41 catalyst:

$$HCHO_{(a)} + O + Ag_{(s)} \rightarrow H_2CO_2-Ag_{(a)} \qquad (1-2)$$

$$HCHO_{(a)} + OH + Ag_{(s)} \rightarrow HCOO-Ag_{(a)} + 2H \qquad (2)$$

$$HCOO-Ag_{(a)} + H \rightarrow CO-Ag_{(a)} + H_2O_{(g)} \qquad (3)$$

$$CO-Ag_{(a)} + O \rightarrow CO_{2(g)} \qquad (4)$$

$$2H_2CO_{2(a)} \rightarrow HCOO_{(a)} + H_3CO_{(a)} \qquad (5)$$

$$HCOO_{(a)} \rightarrow CO_{2(a)} + H_{(a)} \qquad (6)$$

$$2H_{(a)} \rightarrow H_{2(g)} \qquad (7)$$

Firstly, adsorbed HCHO was oxidized into DOM species ($H_2CO_{2(a)}$) in both pure MCM-41 and Ag/MCM-41 (Step (1-2)). The formate ad-species formation would consume surface OH group in the presence of the particular silver-oxygen structure ($Ag_{(s)}$) at room

temperature in the HCHO catalytic oxidation reaction (Step (2)). In addition, heating up also resulted in the disproportionation of DOM into formate *via* a Cannizzaro-type mechanism (Step (5)). Next, the formate (HCOO—$Ag_{(a)}$) formed on the surface of the particular silver-oxygen structure decomposed into adsorbed CO—$Ag_{(a)}$ (Step (3)). And the adsorbed CO was finally oxidized by oxygen into gas phase CO_2 (Step (4)). Importantly, there were two ways for formate species formation: (1) direct reaction from HCHO and (2) Cannizzaro-type mechanism by DOM species. And there also existed two ways for gas phase CO_2 formation: (1) formate dissociated into CO followed by CO oxidized into CO_2 and (2) formate was directly oxidized into CO_2 (Step (6)). At low temperature, the formation rate of formate species was far greater than the decomposition rate of formate to CO_2, which resulted in the formate spawning. With the increase of the temperature, CO_2 became the staple products. On the basis of the above discussion, the formation and decomposition capability of formate controlled the process of HCHO oxidation over Ag catalysts.

The HCHO catalytic oxidation reaction path on the supported noble metal catalysts, such as Pt, Au and Ag and so on, seems to show some difference in the intermediates transformation, including dioxymethylene (DOM), formate and CO ad-species. Over the supported Pt catalysts, the adsorbed HCHO was firstly oxidized into DOM then to formate species [20], which was also found in our pathways of (1-2) and (5) on Ag/MCM-41 catalysts. The adsorbed HCHO could be oxidized by the surface oxygen of the catalyst to directly form formate speices on Au/CeO$_2$ catalysts [38]. Liu et al. [13] found that the catalytic conversion of HCHO into CO_2 and H_2O over 3DOM Au/CeO$_2$ catalyst was experienced in two processes catalyzed by ionic Au^{3+} and metallic Au^0 respectively, in which ionic state Au^{3+} showed higher catalytic activity. In our paper, the formation of the formate ad-species was found to be not only derived from the $HCHO_{(a)}$ dissociation adsorption along with the —OH consumption but also from the disproportionation of DOM active ad-species. In addition, it was thought that CO was one of the most important intermediates and its formation and oxidation capability also played the significant effect on the HCHO oxidation. These differences for our silver catalysts with other noble catalysts could be ascribed to the unique silver-oxygen interaction and the interface role with the MCM-41, which will be further investigated in the near future.

5. Conclusions

In this study, the reaction mechanism of HCHO adsorption and oxidation was systematically investigated over Ag/MCM-41 catalysts by *in situ* FT-IR and HCHO-TPSR methods. HCHO-TPSR experiments showed that the Ag catalyst pretreated with O$_2$ at 500 °C was highly active for HCHO oxidation compared with H$_2$-pretreated Ag catalysts. The DOM, formate and CO species were found to be the main intermediates for HCHO oxidation on Ag/MCM-41 by *in situ* FT-IR. Importantly, the formation of formate and CO were both strengthened due to the presence of the particular silver-oxygen structure (subsurface oxygen), which finally promoted the HCHO oxidation reaction over Ag/MCM-41 catalysts. Additionally, the formation of the formate ad-species was also found to be not only derived from the HCHO dissociation adsorption along with the —OH consumption but also from the disproportionation of DOM active ad-species. The formation of formate and

reaction rates for HCHO catalytic oxidation showed the positive linear relationship on the Ag catalysts.

References

[1] H. Wang, C.Z. He, L.Y. Huai, J.Y. Liu, Journal of Physical Chemistry C 116 (2012) 10639–10648.
[2] A. Montoya, B.S. Haynes, Journal of Physical Chemistry A 113 (2009) 8125–8131.
[3] C. Zhang, H. He, Catalysis Today 126 (2007) 345–350.
[4] S.S. Kim, K.H. Park, S.C. Hong, Applied Catalysis A 398 (2011) 96–103.
[5] H. Huang, D.Y.C. Leung, Journal of Catalysis 280 (2011) 60–67.
[6] T. Kecskes, J. Rasko, J. Kiss, Applied Catalysis A 273 (2004) 55–62.
[7] C. Ma, D. Wang, W. Xue, B. Dou, H. Wang, Z. Hao, Environmental Science and Technology 45 (2011) 3628–3634.
[8] Y. Shen, X. Yang, Y. Wang, Y. Zhang, H. Zhu, L. Gao, M. Jia, Applied Catalysis B 79 (2008) 142–148.
[9] C.F. Mao, M.A. Vannice, Journal of Catalysis 154 (1995) 230–244.
[10] W.J. Shen, X.F. Tang, J.L. Chen, Y.G. Li, Y. Li, Y.D. Xu, Chemical Engineering Journal 118 (2006) 119–125.
[11] M.A. Barteau, M. Bowker, R.J. Madix, Surface Science 94 (1980) 303–322.
[12] B. Liu, Y. Liu, C. Li, W. Hu, P. Jing, Q. Wang, J. Zhang, Applied Catalysis B 127 (2012) 47–58.
[13] B. Liu, C. Li, Y. Zhang, Y. Liu, W. Hu, Q. Wang, L. Han, J. Zhang, Applied Catalysis B 111–112 (2012) 467–475.
[14] G. Busca, J. Lamotte, J.C. Lavalley, V. Lorenzelli, Journal of the American Chemical Society 109 (1987) 5197–5202.
[15] R.I. Masel, J.J. Foster, Industrial and Engineering Chemistry Research 26 (1987) 2557–2558.
[16] H. Idriss, K.S. Kim, M.A. Barteau, Surface Science 262 (1992) 113–127.
[17] G. Busca, V. Lorenzelli, Journal of Catalysis 66 (1980) 155–161.
[18] D. Chen, Z. Qu, S. Shen, X. Li, Y. Shi, Y. Wang, Q. Fu, J. Wu, Catalysis Today 175 (2011) 338–345.
[19] Z.P. Qu, M.J. Cheng, W.X. Huang, X.H. Bao, Journal of Catalysis 229 (2005) 446–458.
[20] C. Zhang, H. He, K.I. Tanaka, Applied Catalysis B 65 (2006) 37–43.
[21] T. Kecskes, J. Rasko, J. Kiss, Applied Catalysis A 268 (2004) 9–16.
[22] J. Rasko, T. Kecskes, J. Kiss, Journal of Catalysis 226 (2004) 183–191.
[23] G.J. Millar, J.B. Metson, G.A. Bowmaker, R.P. Cooney, Journal of Catalysis 147 (1994) 404–416.
[24] D. Sodhi, M.A. Abraham, J.C. Summers, Journal of the Air and Waste Management Association 40 (1990) 352–356.
[25] J. Rasko, T. Kecskes, J. Kiss, Journal of Catalysis 224 (2004) 261–268.
[26] R.W. McCabe, D.F. McCready, Chemical Physics Letters 111 (1984) 89–93.
[27] A.G. Sault, R.J. Madix, Surface Science 176 (1986) 415–424.
[28] J.J. Spivey, Industrial and Engineering Chemistry Research 26 (1987) 2165–2180.
[29] X. Tang, C. Junli, L. Yonggang, L. Yong, X. Yide, W. Shen, Chemical Engineering Journal 118 (2006) 119–125.
[30] D. Chen, Z. Qu, W. Zhang, X. Li, Q. Zhao, Y. Shi, Colloids and Surfaces A: Physicochemical and Engineering Aspects 379 (2011) 136–142.
[31] G.B. Hoflund, Z.F. Hazos, G.N. Salaita, Physical Review B 62 (2000) 11126–11133.
[32] M. Richter, M. Langpape, S. Kolf, G. Grubert, R. Eckelt, J. Radnik, M. Schneider, M.M. Pohl, R. Fricke, Applied Catalysis B 36 (2002) 261–277.
[33] L. Jin, K. Qian, Z.Q. Jiang, W.X. Huang, Journal of Molecular Catalysis A 274 (2007) 95–100.
[34] A. Yin, C. Wen, W.L. Dai, K. Fan, Applied Catalysis B 108–109 (2011) 90–99.
[35] X. Zhang, Z. Qu, F. Yu, Y. Wang, Journal of Catalysis 297 (2013) 264–271.
[36] Z. Qu, W. Huang, M. Cheng, X. Bao, Journal of Physical Chemistry B 109 (2005) 15842–15848.
[37] J. Xue, X. Wang, G. Qi, J. Wang, M. Shen, W. Li, Journal of Catalysis 297 (2013) 56–64.
[38] B.B. Chen, C. Shi, M. Crocker, Y. Wang, A.M. Zhu, Applied Catalysis B 132–133 (2013) 245–255.